RESEARCH ARTICLE

Figures and figure supplements

Diversity and evolution of cerebellar folding in mammals

Katja Heuer *et al*.

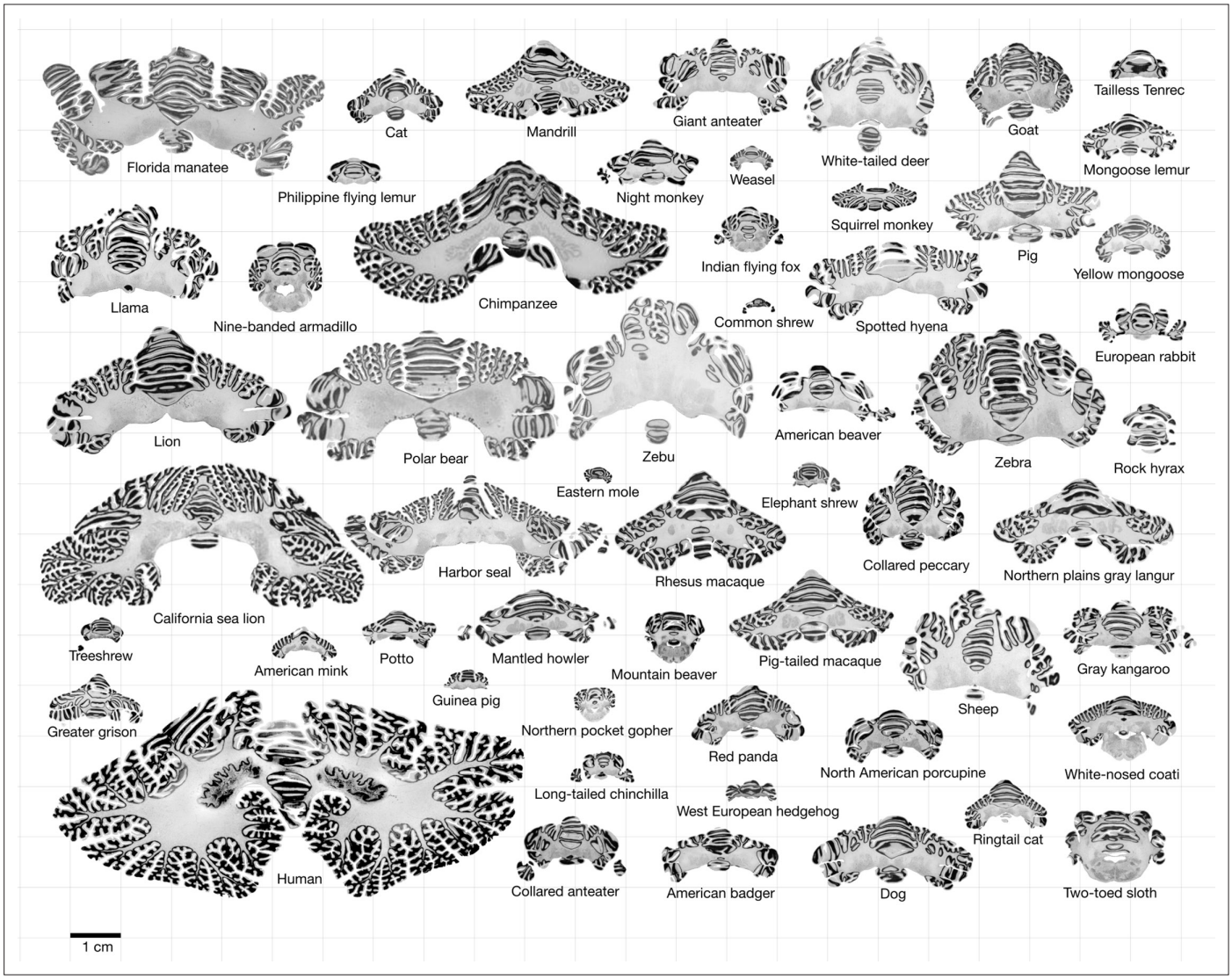

Figure 1. Data. All coronal cerebellar mid-sections for the different species analysed, at the same scale. This dataset is available online for interactive visualisation and annotation: https://microdraw.pasteur.fr/project/brainmuseum-cb. Image available at https://doi.org/10.5281/zenodo.8020178.

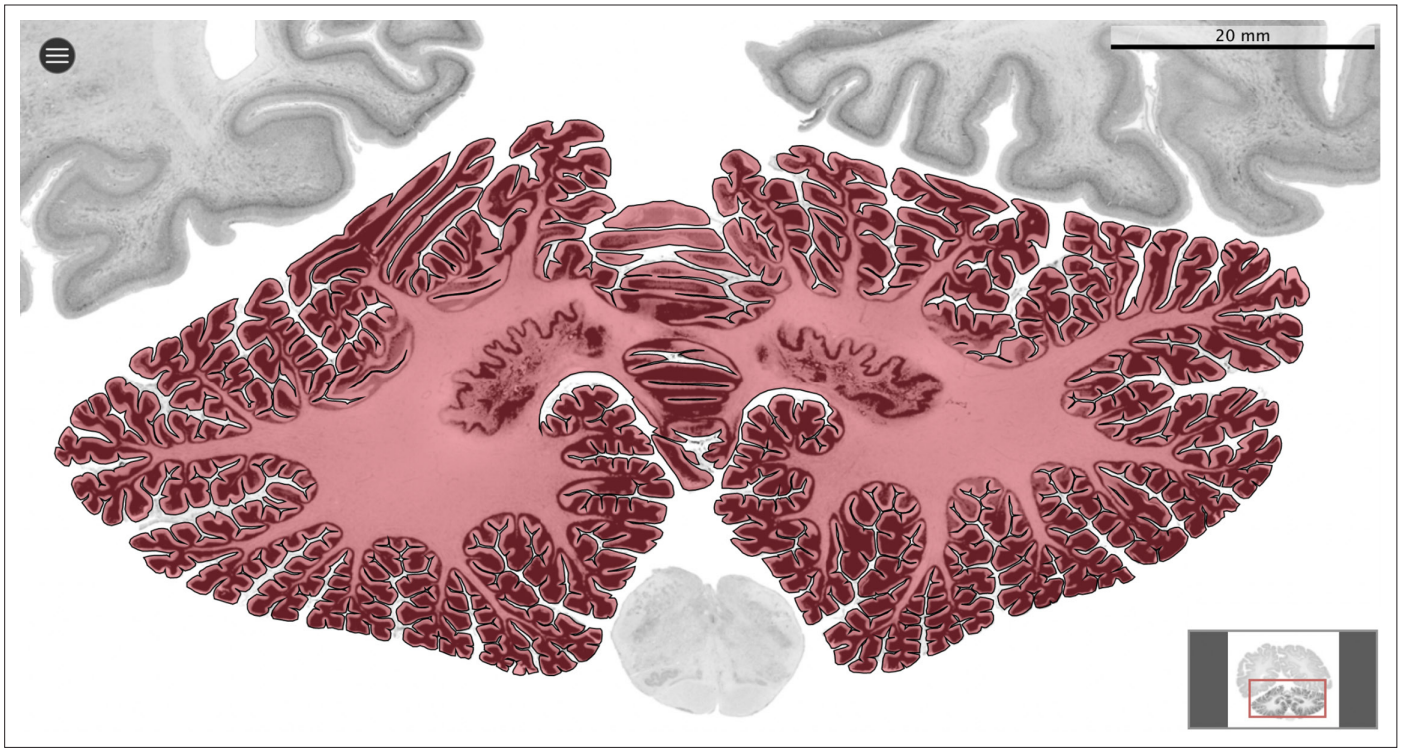

Figure 2. Segmentation. All datasets were indexed in our collaborative Web application MicroDraw (https://microdraw.pasteur.fr) to interactively view and annotate the sections. The contour of the cerebellum was drawn manually using MicroDraw (black contour). The example image shows the human cerebellum from the BigBrain 20 µm dataset (***Amunts et al., 2013***).

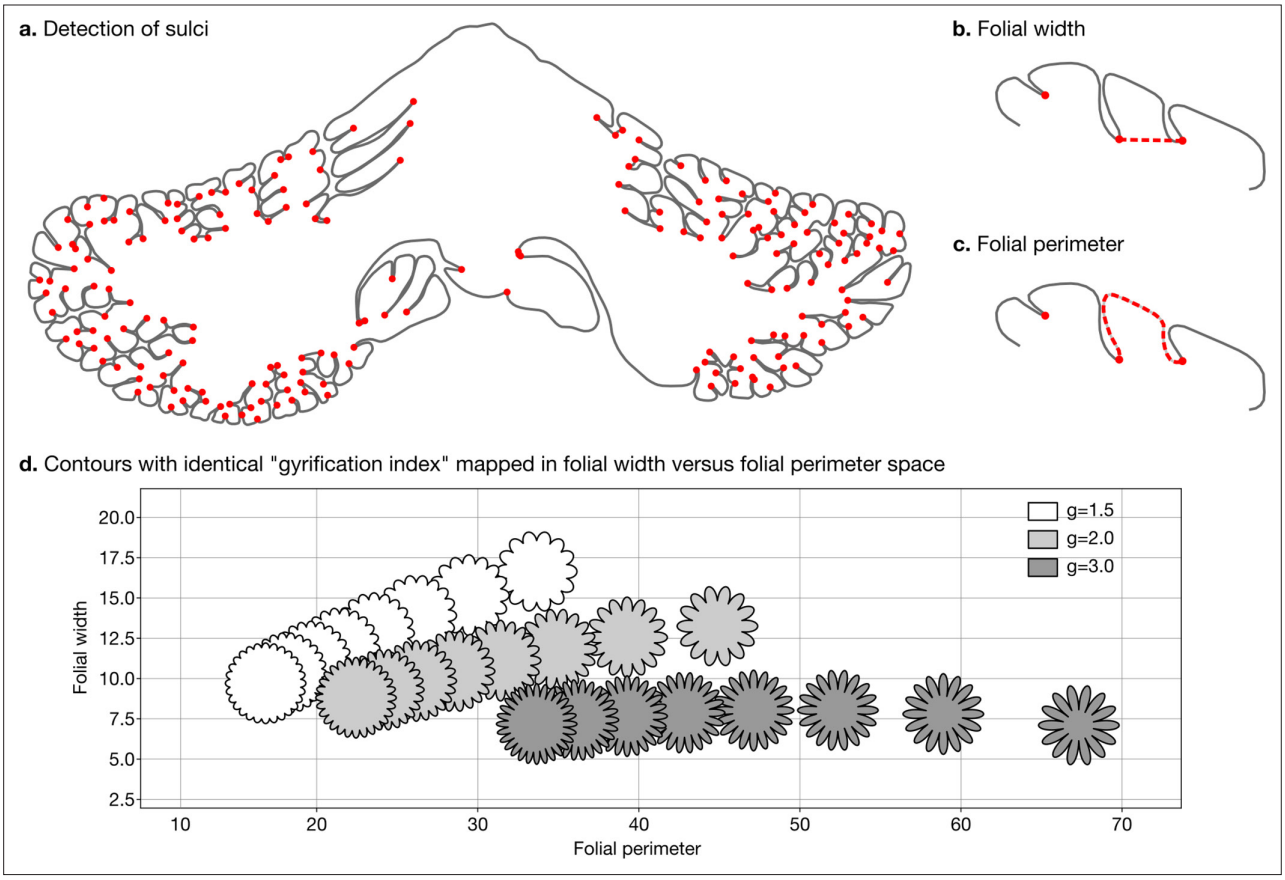

Figure 3. Detection of sulci and measurement of folial width and perimeter. Sulci were automatically detected using mean curvature filtered at different scales (**a**). From this, we computed folial width (**b**) and folial perimeter (**c**). (**d**) Folial width and perimeter allow to distinguish folding patterns with the same gyrification index. The three rows of contours have the same gyrification index (top g=1.5, middle g=2.0, bottom g=3.0), however, the gyrification index does not allow distinguishing between contours with many shallow folds and those with few deep ones.

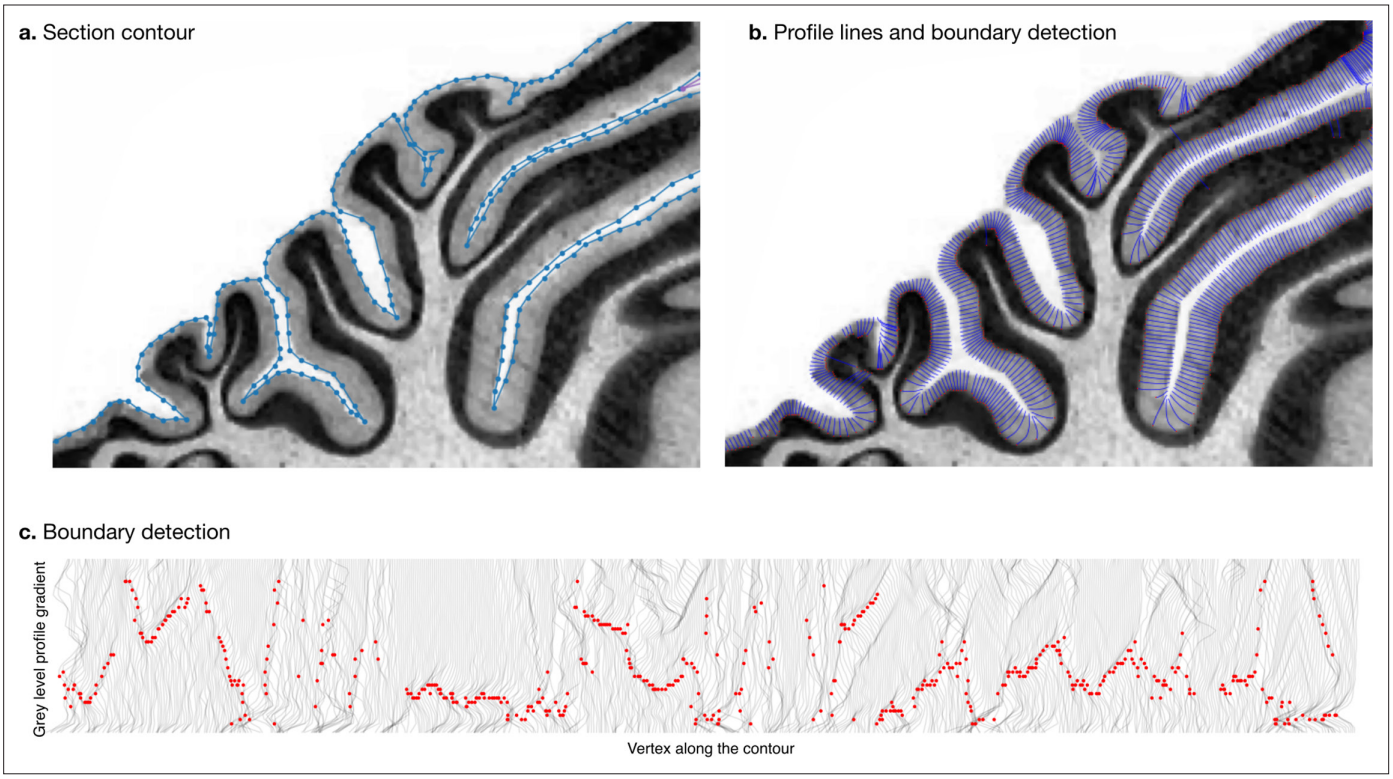

Figure 4. Measurement of molecular layer thickness. The thickness of the molecular layer was measured automatically from the surface segmentation. (**a**) Zoom into a manually annotated surface contour. (**b**) Automatically computed profile lines. (**c**) Grey level profile gradients and border detection for the whole slice. Red dots indicate detected borders (maximum gradient).

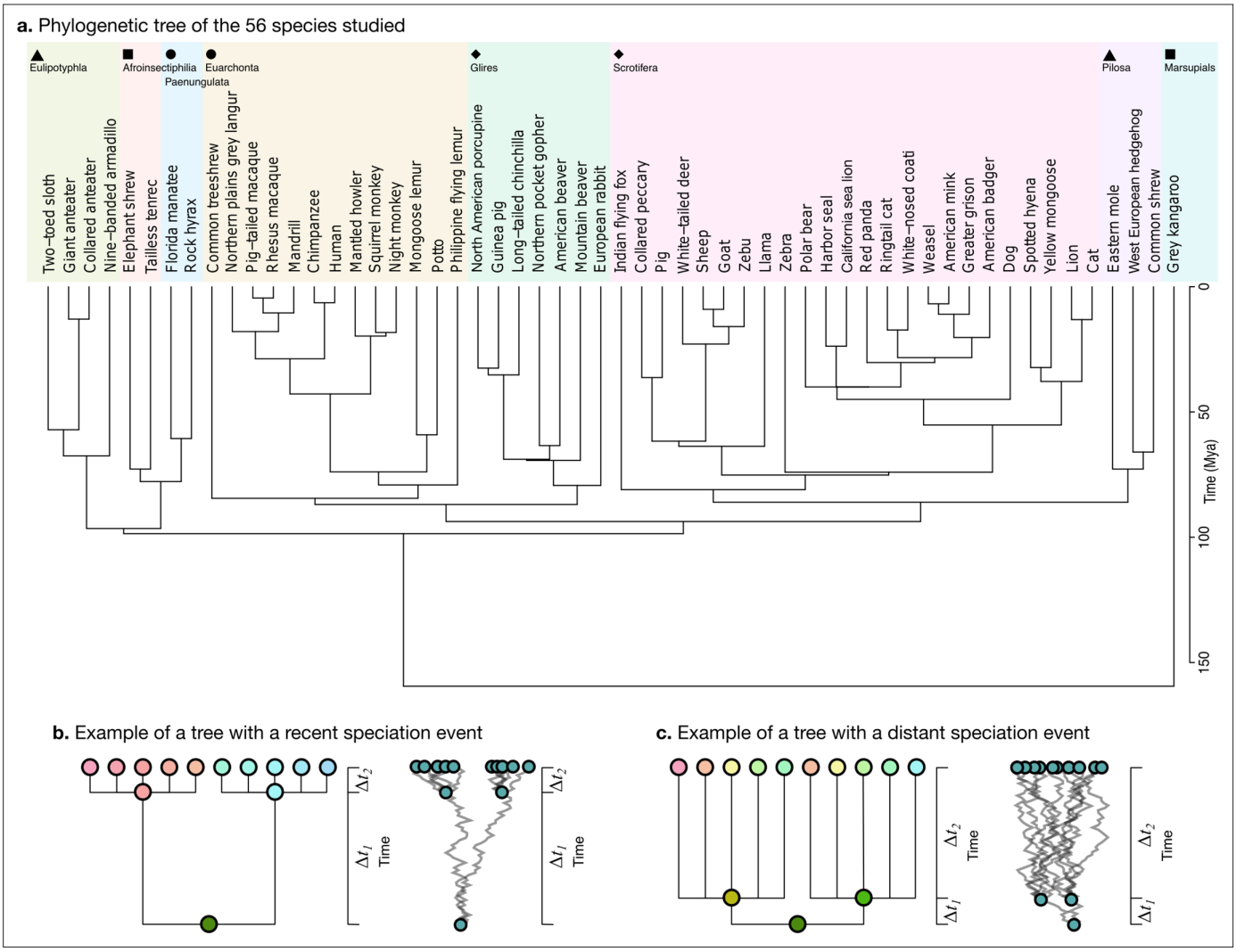

Figure 5. Phylogenetic tree. (**a**) The phylogenetic tree for 56 species used in our study was downloaded from the TimeTree website (http://www.timetree.org, ***Kumar et al., 2017***) and coloured in eight groups based on hierarchical clustering of the tree. (**b**) Not accounting for phylogenetic information can lead to misinterpretations of cross-species relationships. Consider the case of eight species descending from two recent ancestors as in the tree ($\Delta t_2 \ll \Delta t_1$, adapted from ***Felsenstein, 1985***). Even if their phenotypes evolved randomly (Brownian motion [BM] process in the phenogram to the right), they will seem to be more similar within each group. (**c**) If the time of split from their common ancestor were more distant ($\Delta t_2 \gg \Delta t_1$), this difference would not exist. Real phylogenetic trees embed a complex hierarchical structure of such relationships.

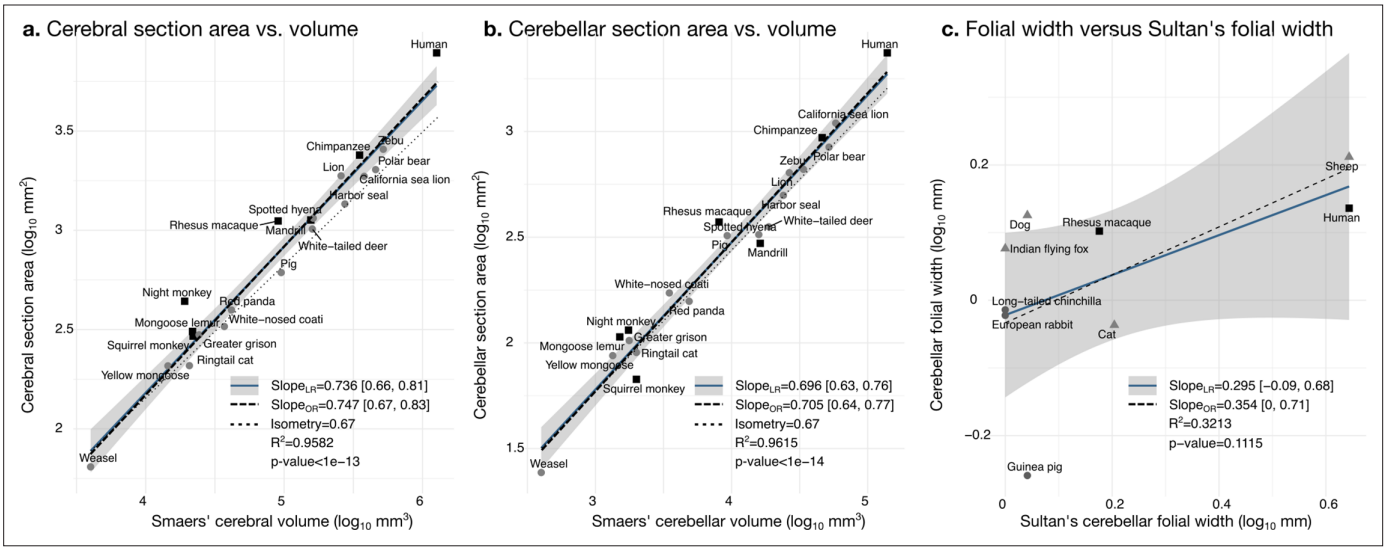

Figure 6. Validation of neuroanatomical measurements. Comparison of our cortical section area measurement (**a**) and cerebellar section area (**b**) with volume measurements from ***Smaers et al., 2018***. (**c**) Comparison of our folial width measurement with folial width from ***Sultan and Braitenberg, 1993***. The folial width measurement reported by Sultan and Braitenberg, which may include several folia, do not correlate significantly with our measurements (two-tailed p=0.112). LR: linear regression with 95% confidence interval in grey. OR: orthogonal regression.

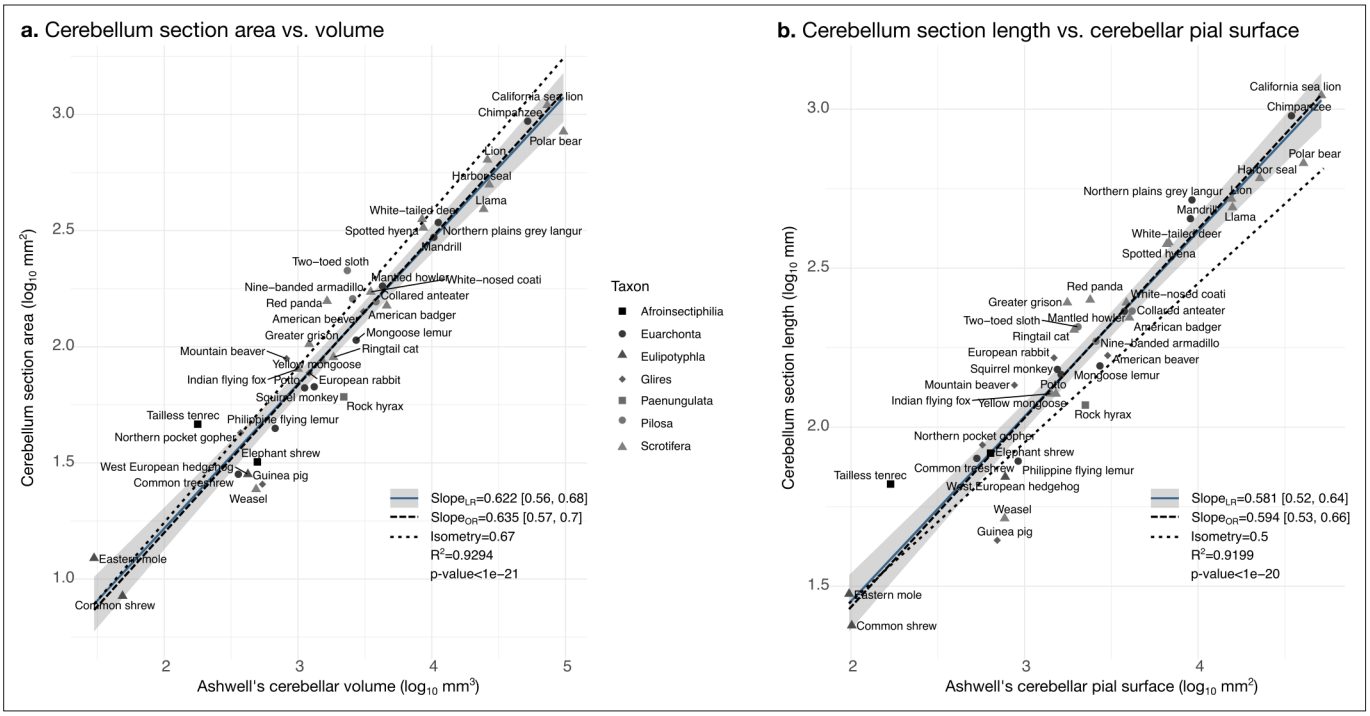

Figure 6—figure supplement 1. Validation of neuroanatomical measurements: correlation with measurements in ***Ashwell, 2020***. Comparison of our cerebellar section area measurement (**a**) and cerebellar section length (**b**) with cerebellar volume and surface measurements from ***Ashwell, 2020***. Measurements correlate significantly (two-tailed p<1e-20). LR: linear regression with 95% confidence interval in grey. OR: orthogonal regression.

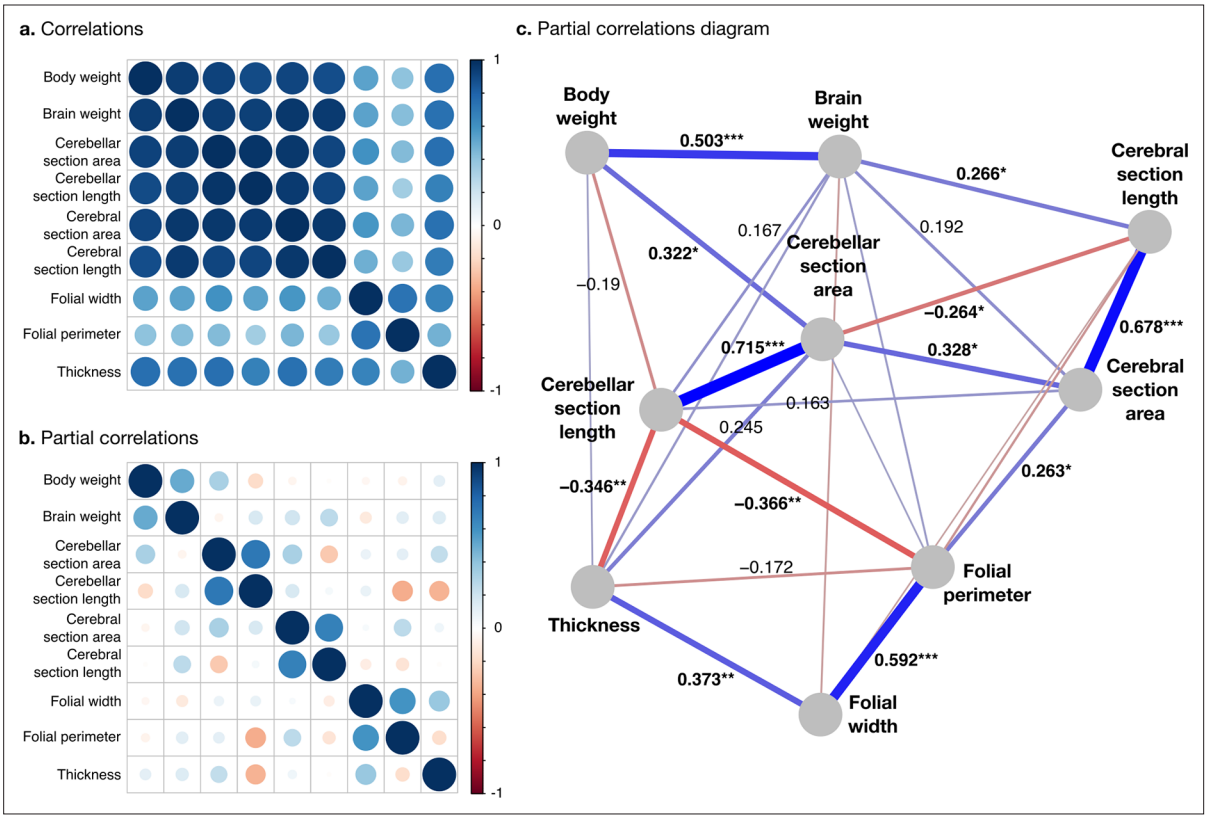

Figure 7. Correlation structure. (**a**) Correlation matrix among all phenotypes (all values $\log_{10}$ transformed). (**b**) Partial correlation matrix. (**c**) Graph representation of the strongest positive (red) and negative (blue) partial correlations. All correlations are conditional to phylogenetic tree data. Partial correlation significance is indicated by asterisks, *** for p<0.001, ** for p<0.01, * for p<0.05. Partial correlations without asterisks are not significant.

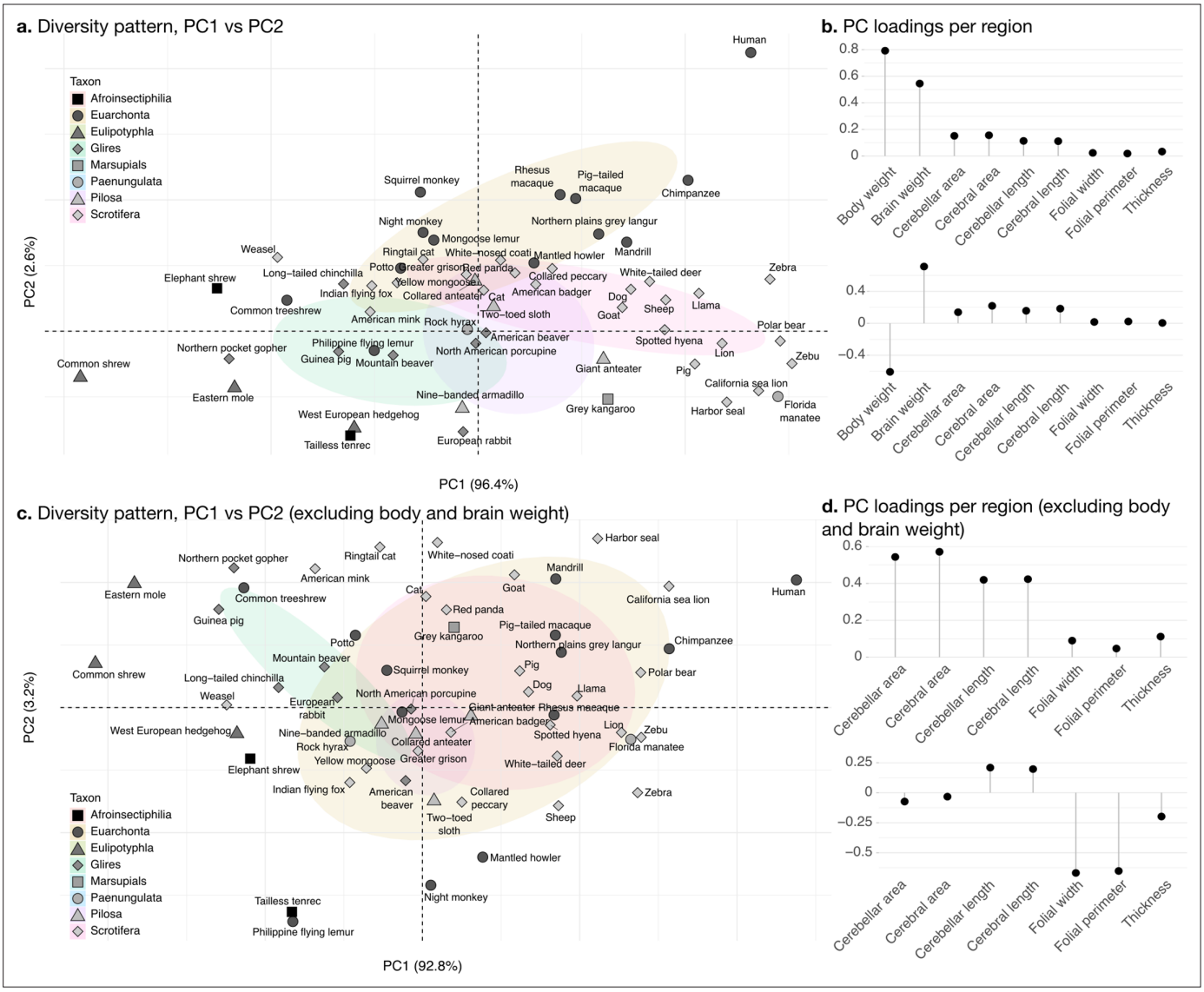

Figure 8. Phylogenetic principal component analysis. Primates, and especially humans, show particularly large brains given their body size. (**a**) Pattern of neuroanatomical diversity (PC1 vs. PC2), including body and brain weight. (**b**) Loadings of the PC1 and PC2 axes displayed in panel a. (**c**) Pattern of neuroanatomical diversity (PC1 vs. PC2), excluding body and brain weight. (**d**) Loadings of the PC1 and PC2 axes displayed in panel c.

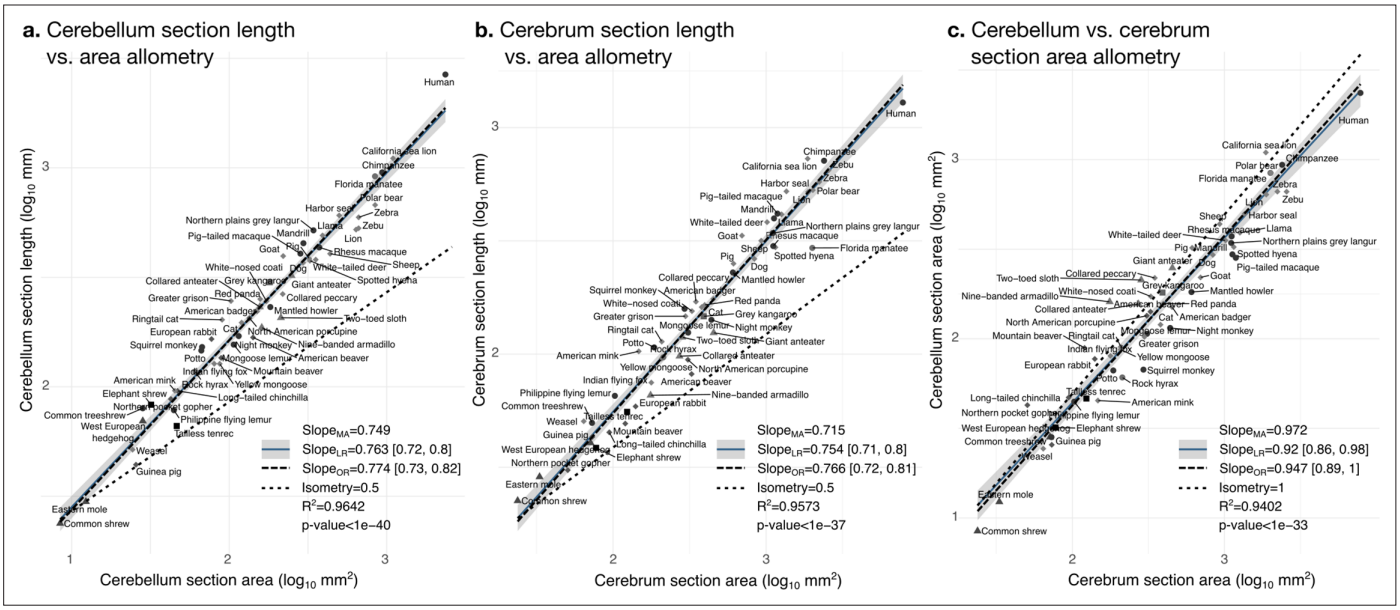

Figure 9. Cerebellum and cerebrum folding and allometry. The cerebellar and cerebral cortices are disproportionately larger than their volumes, as shown by their hyper-allometry. The cerebellum is slightly but statistically significantly hypo-allometric compared to the cerebrum. (**a**) Allometry of cerebellum section length vs. cerebellum section area. (**b**) Allometry of cerebrum length vs. cerebrum section area. (**c**) Allometry of cerebellum section area vs. cerebrum section area. MA: multivariate allometry. LR: linear regression with 95% confidence interval in grey. OR: orthogonal regression.

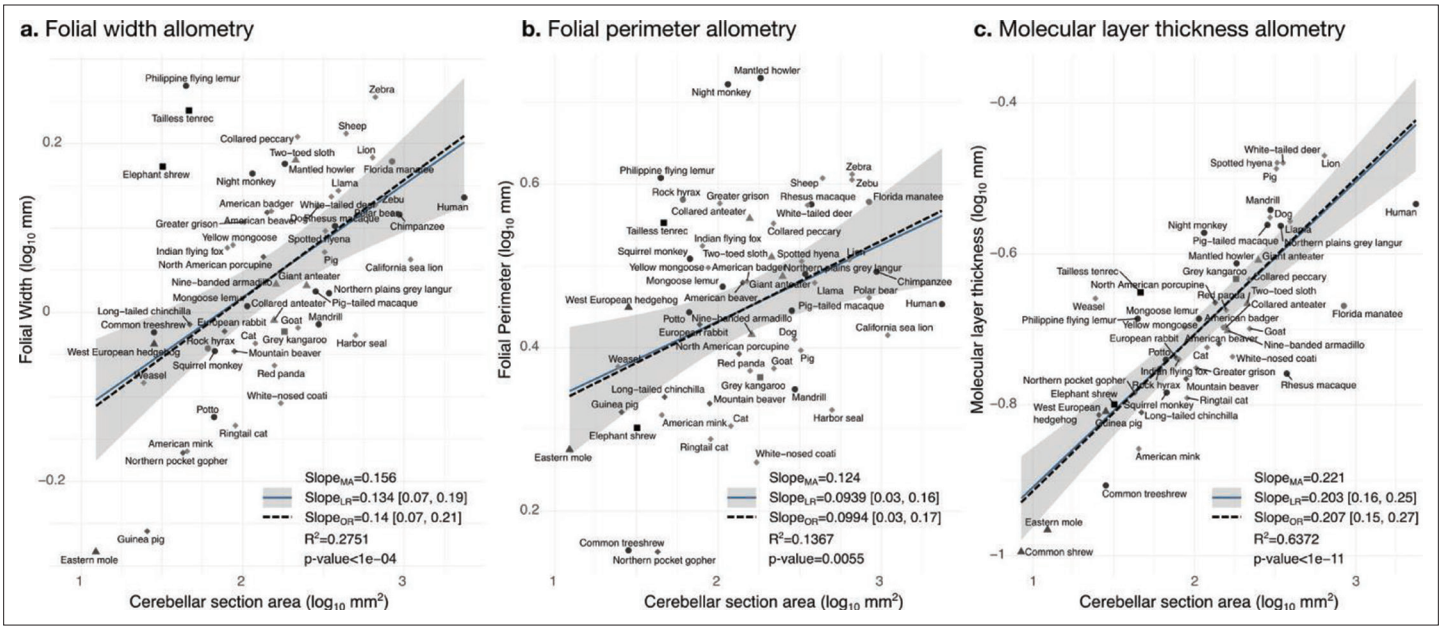

Figure 10. Allometry of folial width, perimeter, and molecular layer thickness. The geometry of cerebellar folia and molecular layer thickness were largely conserved when compared with changes in total cerebellar size, as revealed by the small allometric slopes. (**a**) Allometry of folial width vs. cerebellar section area (two-tailed p<1e-5). (**b**) Allometry of folial perimeter vs. cerebellar section area (two-tailed p=0.005). (**c**) Allometry of the thickness of the molecular layer vs. cerebellar section area (two-tailed p<1e-12). MA: multivariate allometry. LR: linear regression with 95% confidence interval in grey. OR: orthogonal regression.

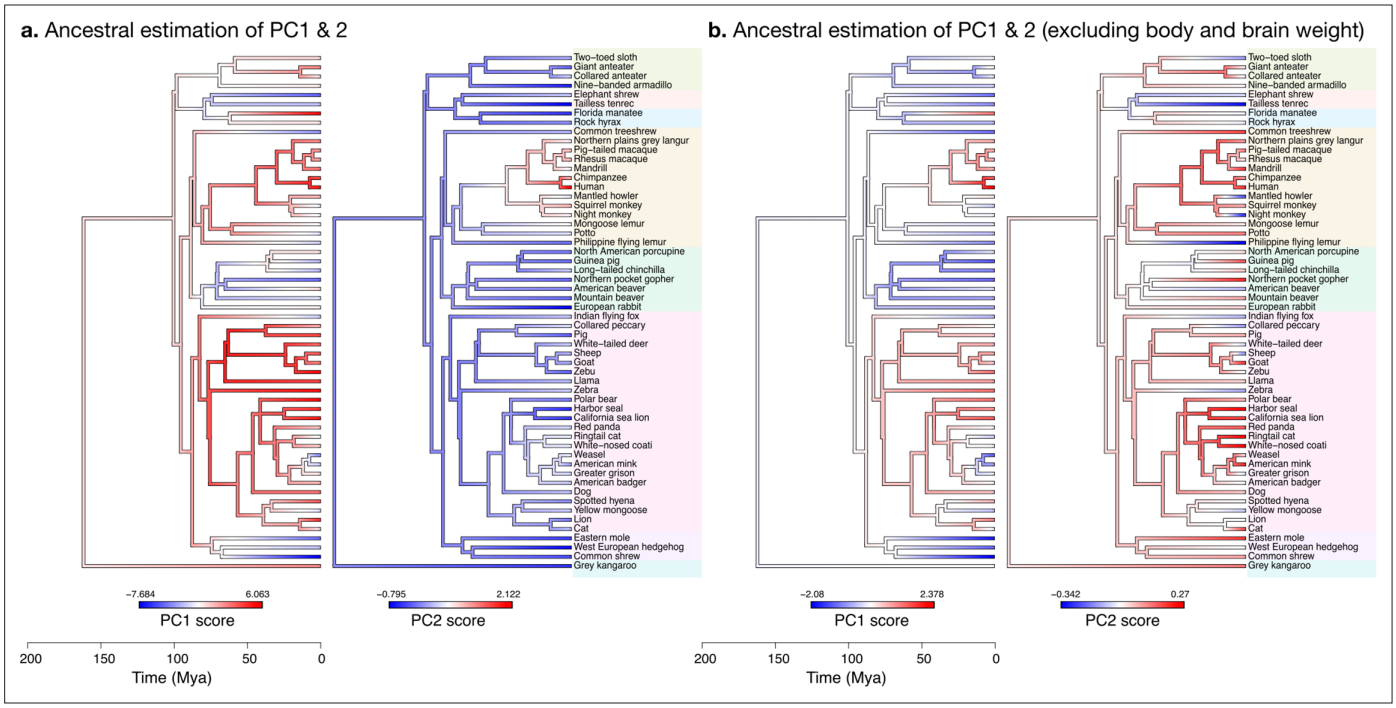

Figure 11. Estimation of ancestral neuroanatomical diversity patterns. Our analyses show a concerted change in body and brain size, and specific increase in cerebral and cerebellar volume in primates concomitant with an increased number of smaller folia. (**a**) Ancestral estimation of PC1 and PC2 for neuroanatomical variables plus brain volume. PC1 captures 96.4% of the variance, PC2 captures 2.4%. (**b**) Ancestral estimation of PC1 and PC2 for neuroanatomical variables, without brain volume. PC1 captures 91.4% of phenotypic variance, PC2 captures 3.6%.